CrossMark

Using multi-model ensembles to improve the simulated effects of land use/cover change on temperature: a case study over northeast China

**Xianliang Zhang[1,2] · Zhe Xiong[3] · Xuezhen Zhang[4] · Ying Shi[5] · Jiyuan Liu[4] ·
Quanqin Shao[4] · Xiaodong Yan[2]**

Abstract Rather than simulating the effects of land use and land cover change (LUCC) on the climate using one climate model, as in many previous studies, three regional climate models (Regional Climate Model, version 3; the Weather Research and Forecasting model; and the Regional Integrated Environmental Model System) were used in the present study to simulate changes in temperature due to LUCC. Two experiments (CTL and NE) were designed and run using the three regional climate models. The CTL experiment was used to compare the simulations of the different models and served to illustrate the improvement that could be achieved as a result of employing a multi-model ensemble. The NE experiment was used to evaluate the changes in temperature caused by LUCC in northeast China between 1981 and 2000. The results of the CTL simulations showed that changes in temperature were simulated well by the three regional climate models; however, the simulated temperatures were different, dependent on the model used. The multi-model ensembles [the arithmetic ensemble mean (AEM) and Bayesian model averaging (BMA)] attained better results than any individual model. Of the two ensemble methods, BMA performed better than the AEM. The effects of LUCC on the climate in northeast China were assessed by the differences between the CTL and NE simulations for every RCM and the ensemble simulations. The BMA simulations produced more reasonable results than the other simulations. Based on the results, we can state with some confidence that LUCC in northeast China over the 20-year period studied caused a decrease in temperature, because of an expansion of arable land.

Keywords Land use/cover change · Regional climate model · Multi-model ensemble · Bayesian model averaging

1 Introduction

Land use and land cover change (LUCC) reflects the influences of human activities on the Earth's surface. According to a U.S. National Aeronautics and Space Administration (NASA) report, one-third to one-half of the global land surface has been transformed by human development. Land use change has significant influences on the environment, including those on water use (Foley et al. 2005; Tian et al. 2011), aspects of the biogeochemical cycle such as carbon dynamics (Tian et al. 2003), and especially the climate (Kalnay and Cai 2003; Cai and Kalnay 2004). Significant changes in land use and land cover alter the physical properties of the land surface, such as the surface albedo, roughness and the Bowen ratio, which also indirectly alter the climate. Many studies have documented the impacts of LUCC on the climate (e.g. Avissar and Pielke 1989; Nobre et al. 1991; Bounoua et al. 2002; Pielke et al. 2002; Trenberth 2004; Pielke 2005). For instance, replacing tropical

✉ Xiaodong Yan
  yxd@bnu.edu.cn

1 College of Forestry/Research Station of Liaohe-River Plain Forest Ecosystem, CFERN, Shenyang Agriculture University, Shenyang 110866, China

2 State Key Laboratory of Earth Surface Processes and Resource Ecology, Beijing Normal University, Beijing 10087, China

3 Key Laboratory of Regional Climate-Environment for East-Asia, Institute of Atmospheric Physics, Chinese Academy of Sciences, Beijing, China

4 Institute of Geographic and Natural Resources Research, Chinese Academy of Sciences, Beijing, China

5 National Climate Center, China Meteorological Administration, Beijing, China

rainforest with pasture has led to a warmer and drier climate (Mcguffie et al. 1995; Zhang et al. 1996, 2001), and desertification could reduce precipitation (Xue and Shukla 1993; Xue 1996). These studies illustrate that changes in land use and land cover have significant impacts on climate change.

The current vegetation of China has been heavily influenced by human activities, due to its long history of agriculture and high population. With rapid development in China, land use and land cover has experienced great change in the 20 years from 1981 to 2000. In particular, marked LUCCs have occurred in southern (reforestation around the Yangtze River), eastern (forest changed to cropland) and central (grassland changed to cropland) China (Liu et al. 2002, 2003). The most obvious LUCC in these regions has been the transformation of large areas of forest and grassland into arable land. Clearly, eastern parts of China have experienced substantial LUCC in recent years; as a result, this region was selected as the research area in the present study.

Regional climate models (RCMs), which are generally used to simulate regional climate and its changes (Giorgi et al. 1994; Gutowski et al. 2003, 2004, 2010), can also be used to simulate the effects of regional land changes on climate. In fact, the effects of LUCC on the regional climate in China have previously been investigated using RCMs, based on single-model simulations (Gao et al. 2003; Zhang et al. 2005, 2011; Zhang and Gao 2009). However, different RCMs produce different results, even when modeling the climate of the same region (Déqué et al. 2012; Fu et al. 2005; Mearns et al. 2012). Thus, there is large uncertainty when climate effects are simulated by any one RCM.

It is well known that multi-model ensemble (MME) methods can be used to integrate results of different models and produce better results than any one individual model; many studies have demonstrated that an ensemble of different simulations from global climate models produces more accurate results than separate single-model outputs (e.g. Gates et al. 1999; Kirtman and Min 2009; Weisheimer et al. 2009; Annan and Hargreaves 2010; Kirtman et al. 2013). Therefore, it is worth investigating whether an ensemble of RCMs can produce more accurate results than a single RCM when simulating the effects of LUCC on climate.

The most commonly used and conventional MME method is the arithmetic ensemble mean (AEM). The AEM integrates the simulated values of multiple models and reduces the simulated error by offsetting the positive and negative biases of different models (Hagedorn et al. 2005). However, the errors of the individual models cannot cancel each other out completely (Reifen and Toumi 2009). Accordingly, weighted ensemble methods have been used to provide better results than the AEM (Zhang and Yan 2014). Of these methods, Bayesian model averaging

(BMA) has been widely used as an effective tool in many studies; it has been proven that much better results can be obtained using BMA, compared to AEM or any individual model (e.g. Duan et al. 2007; Raftery et al. 2005; Sloughter et al. 2007).

To the best of our knowledge, there have been no studies conducted in which the effects of LUCC on climate have been examined using a multi-RCM ensemble. Therefore, the aim of the present reported study was to compare the effects of LUCC on the climate in eastern China, as simulated by three RCMs, and investigate the possibility of improving the results by using a multi-RCM ensemble. Within this overall aim, the main goals of the study were to (1) compare the climate effects of LUCC simulated by different RCMs, and (2) calculate the MME simulations, using AEM and BMA, and compare the improvement in model simulations when using the MME approaches.

2 Data and methods

2.1 Model descriptions

To compare the effects of LUCC on climate, as simulated by different RCMs, three RCMs [Regional Climate Model, version 3 (RegCM3); the Weather Research and Forecasting (WRF) model; and the Regional Integrated Environmental Model System (RIEMS)] were used in this study. Brief descriptions of these models are as follows:

2.1.1 Regional Climate Model, version 3

RegCM3 (Giorgi et al. 1993a, b; Pal et al. 2007), developed by the International Center for Theoretical Physics, is a third-generation regional scale climate model, derived from the Mesoscale Model, version 5 (MM5), of the National Center for Atmospheric Research (NCAR)—Pennsylvania State University (PSU). RegCM3 includes the same dynamical core as MM5, the Biosphere–Atmosphere Transfer Scheme (BATS) (Dickinson et al. 1993), radiative transfer package (Kiehl et al. 1996), and the Community Climate Model, version 3 (CCM3). RegCM3 is a primitive equation, sigma vertical coordinate regional climate model. Its vertical resolution is 18 levels, with seven levels below 800 hPa. The documentation and source code of RegCM3 are available at www.ictp.trieste.it/RegCNET/model.html.

RegCM has performed quite well in simulating regional climate change in China (Gao et al. 2002; Wang et al. 2003). Using RegCM, Gao et al. (2003, 2007) conducted a number of investigations into the influence of LUCC on the climate of China. They showed that the annual mean temperature decreased in northeastern and southern China, while it increased in the northwest of China, when the

potential vegetation cover was changed to the current land use. Suh and Lee (2004) revealed a cooling effect in central and northern China when the land use changed from broad-leaf forest to irrigated cropland.

2.1.2 Weather research and forecasting model

The WRF model is a next-generation, regional weather research and forecasting model. It was developed by the NCAR, the National Centers for Environmental Prediction (NCEP) and the Forecast Systems Laboratory, the Air Force Weather Agency, the Naval Research Laboratory, the University of Oklahoma, and the Federal Aviation Administration. The WRF model includes two dynamical cores, a data assimilation system and a software architecture, allowing for parallel computation and system extensibility. Worldwide, scientists from many countries use it for operational weather forecasting, regional climate prediction, air-quality simulation and idealized dynamical studies. A detailed description of the WRF model can be found at http://www.wrf-model.org/index.php.

The WRF model has been effective in simulating regional climate change in China (Zhang et al. 2011). Based on WRF model simulations, Feng et al. (2013) simulated the impacts of urbanization on climate; Wang et al. (2014) showed that replacing shrubland by grassland caused an increase in summer temperature in the northern and southern parts of the Hetao Plain; and Ge et al. (2014) found that the effects of LUCC on climate were stronger in the growing season than in the non-growing season, by comparing the effects of dynamic vegetation on climate with those of fixed vegetation.

2.1.3 Regional integrated environmental model system

RIEMS was developed by the Regional Center for Temperate East Asia, Chinese Academy of Sciences (Fu et al. 2000). The dynamic component of this model is the same as in MM5. RIEMS includes the land surface physics scheme BATS1e (Dickinson et al. 1993), a Kuo–Anthes cumulus parameterization, and a CCM3 radiative transfer package (Kiehl et al. 1996).

RIEMS was mainly designed to model the regional climate of eastern Asia and, as such, it tends to perform well when simulating the regional climate of China (Fu et al. 2005; Xiong et al. 2006; Wang et al. 2013; Zhao 2013). Fu (2003) revealed that human-induced LUCC caused changes in the Asian summer monsoon with RIEMS, while Zhang et al. (2005) showed that the temperature increased over regions of vegetation change, due to land surface degradation in northern China. The regional climate, monsoon systems and ecological engineering have also been shown to be affected by variations in LUCC in western China (Shi and Wang 2003; Wang et al. 2006).

2.2 Experimental design

To reveal the effects of LUCC on climate from 1981 to 2000 in eastern China, two experiments were designed: a control experiment (CTL) and a land use change experiment (exemplified in northeast China; NE). The land cover data used in both experiments were developed by Liu et al. (2005) by integrating imagery of remotely sensed data and geophysical data, and so are more representative of land cover in China than the U.S. Geological Survey (USGS) land cover data. This dataset has a 1 km resolution and uses land use categories defined by Liu et al. (2005). Spatial aggregation and type conversions were performed to change the categories to match the USGS land cover categories, according to the criteria shown in Table 1. In the CTL experiment, land cover data from the year 2000 (Fig. 1) were used as a fixed vegetation parameter. In the NE experiment, the vegetation types from the year 2000 were replaced by the vegetation types present in 1980, in northeast China (the square region in Fig. 1). The CTL simulation and NE simulation used exactly the same simulation domain and period, lateral boundary conditions and settings of physical parameterizations, except for the prescribed land cover parameter.

The CTL and NE simulations were run using the three regional climate models (WRF, RegCM3 and RIEMS). The three RCMs were driven by the same initial and boundary conditions (6-h interval NCEP II reanalysis data). The simulations of the three RCMs covered the 21-year period from 1980 to 2000 and were initialized on 1 January 1980. The first year was used as the spin-up period and is not considered in the analysis.

The simulated domains of the different RCMs (Fig. 1) were roughly located over the same region of China, although their resolutions were different. For RegCM3, the resolution of the horizontal grids was 50 km, and the central point of the domain was (36°N, 116°E), with 159 grid cells in the west–east direction and 128 grid cells in the south–north direction. For the WRF model, the model domain had a central point of (37°N, 117°E), and a horizontal resolution of 30 km, with 95 grid cells in the west–east direction and 139 grid cells in south–north direction. For RIEMS, the model domain had a central point of (36°N, 117.5°E), and a horizontal resolution of 30 km, with 79 grid cells in the west–east direction and 139 grid cells in the south–north direction.

2.3 Multi-model methods

2.3.1 AEM method

The AEM is defined by

$$Y(t) = \frac{1}{K} \sum_{i=k}^{K} F_k(t), \tag{1}$$

Table 1 The rules for spatial aggregation and land use type conversions from the land cover data of Liu et al. (2005) to USGS land cover categories

Liu land use Code	Liu land use category Name/description	USGS Code	USGS category Name
One to one conversion; any single land use (left land side) accounts for more than half of the model grid			
51–53	Building area	1	Urban and built-up land
12	Dry cropland	2	Dry cropland and pasture
11	Irrigated cropland	3	Irrigated cropland and pasture
31–33	Grassland	7	Grassland
22	Shrub	8	Shrub land
41–43	Water body	16	Water body
45–46	Wet land	17	Herbaceous wetland
61–67	Bare land	19	Barren or sparsely vegetated
44	Land ice/snow cover	24	Snow or ice
One to more conversion; total area of land use (left hand side) accounts for more than half of the model grid			
23	Sparse woodland	10	Savanna
24	Cut over land		
More to one conversion; using the vegetation regionalization map to determine forest type and the single type of forest accounts for more than half of the model grid			
21	Forest	11	Deciduous broadleaf forest
		12	Deciduous needleleaf forest
		13	Evergreen broadleaf forest
		14	Evergreen needleleaf forest

Land use categories Description	USGS Code	USGS categories Name
Mixed type of land cover, excluding the above conditions		
Total area of dryland (code 12) and irrigated (code 11) cropland accounts for more than half of the model grid	4	Mixed dryland/irrigated cropland and pasture
Forest (code 21) accounts for more than half of the model grid and no dominant USGS forest could be found	15	Mixed forest
Grassland (code 31–33) and cropland (code 11–12) are the largest two land use types in the model grid	5	Cropland/grassland mosaic
Woodland (code 21–24) and cropland (code 11–12) are the largest two land use types in the model grid	6	Cropland/woodland mosaic
Woodland (code 21–24) and grassland (code 31–33) are the largest two land use types in the model grid	9	Mixed shrubland/grassland

where $Y(t)$ is an ensemble prediction for time t, K is the total number of models, and $F_k(t)$ is a forecast of the kth model for time t.

2.3.2 Bayesian model averaging (BMA)

The BMA method involves updating prior information of a variable based on new available information (Bayes 1763). Suppose that y is a random variable at a future time, the prior information of y is a probability density function

(PDF) $p(y)$. A forecast of y can be made by its relationship with the predictor x, if the new information x is given. The condition distribution $p(y|x)$ is computed as

$$p(y|x) = \frac{p(y)p(x|y)}{p(x)}, \tag{2}$$

where $p(y|x)$ is the posterior distribution of x; the prior distribution $p(y)$ and $p(x)$ are the unconditional distributions of y and x, respectively; and $p(x|y)$ is the likelihood function, which reflects the relationship between y and x.
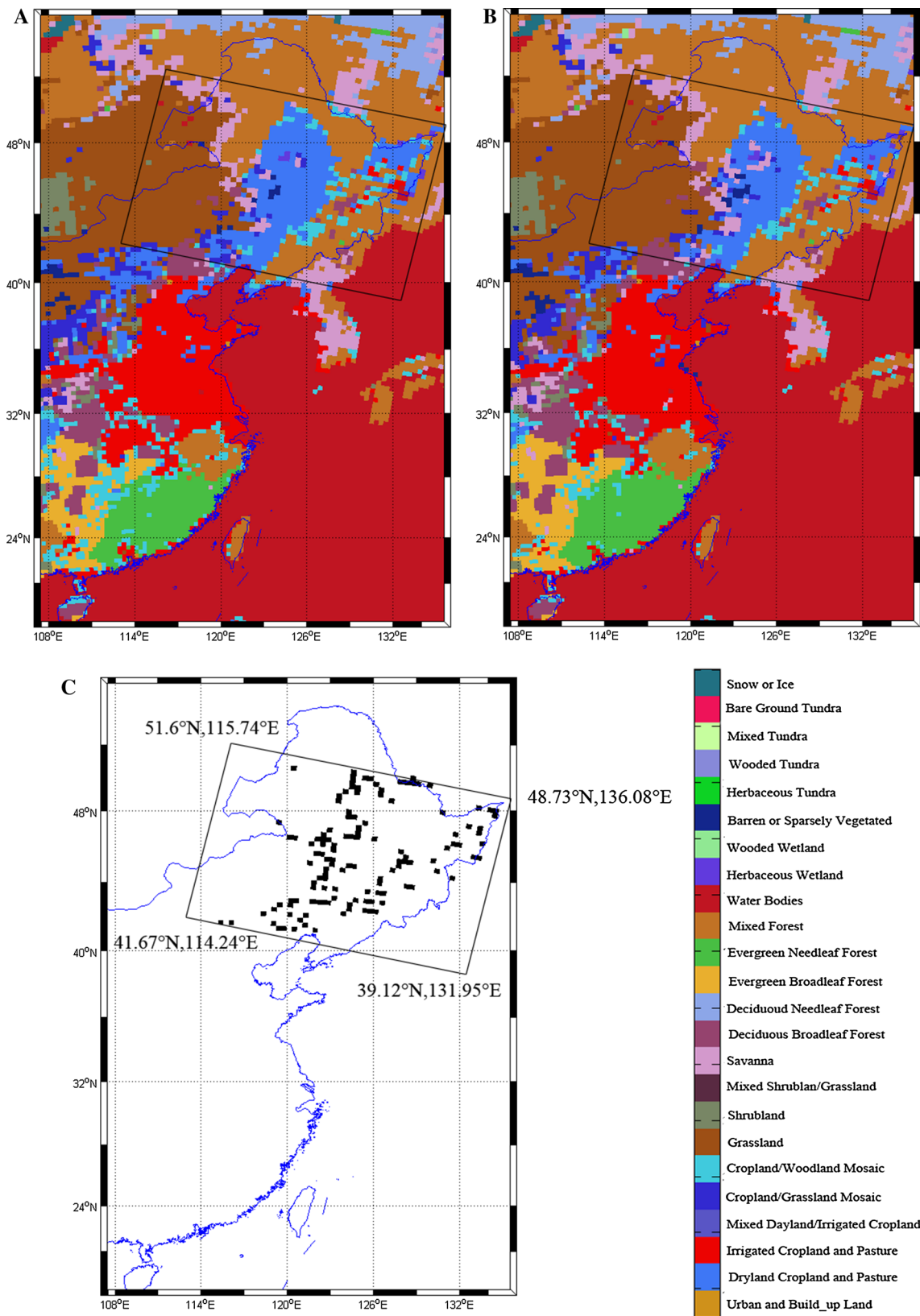
Fig. 1 Land use/cover types in northeast China in **a** 2000 and **b** 1980 and **c** their differences (land use in 2000 minus land use in 1980)

In the case of forecasting y using K predictors $x_1, \ldots, x_K$, the Bayesian forecast PDF $p(y|x_1 \cdots x_K)$ can be given by the BMA, as

$$p(y|x_{1 \ldots} x_k) = \sum_{k=1}^{K} w_k p_k(y|x_k), \qquad (3)$$

where w_k is the weight of the kth model and $p_k(y|x_k)$ is the forecast PDF, based on predictor x_k. The $p_k(y|x_k)$ is the approximate conditional PDF by a normal distribution, centered at a linear function of the predictor, $a_k + b_k x_k$. Therefore, the BMA mean is the conditional expectation of y, given the forecast, so the deterministic BMA ensemble prediction is calculated as

$$E(y|x_{1 \ldots} x_k) = \sum_{k=1}^{K} w_k(a_k + b_k f_k), \qquad (4)$$

where a_k and b_k can be obtained by the regression between the x_k and y in the training period. The weights w_k are calculated using the Expectation–Maximization algorithm (Raftery et al. 2005; Duan et al. 2007; Zhang and Yan 2015).

The BMA ensemble results were calculated with a cross-validation method, to avoid artificial skill. Each year was successively removed from the whole dataset and the remaining years were used to calculate the model and observed statistics. The forecast was then calculated using the statistics for the verification year.

2.4 Analysis of the simulations

Monthly temperature and precipitation can be outputted by the three RCMs. Anomalies of annual mean temperature and total precipitation were calculated to illustrate the model results in the CTL simulations. In the validation step, the CTL simulations were used to evaluate the performances of the three models and their ensemble simulations. The temperature data were verified with Climate Research Unit TS 3.1 temperature data (Harris et al. 2014). The observed temperature at a spatial resolution of $0.5° \times 0.5°$ was used, so the simulated data were interpolated to, and masked with, the observed grid. The biases of the spatial pattern of temperature (mean of 1981–2000) were calculated to illustrate the system bias of each individual RCM and their ensemble simulations; conventional statistics [correlation, bias and root-mean-square error (RMSE)] were used to evaluate the performances of each RCM and their ensemble simulations. Correlation is an important index to test the consistency and similarity between observed and simulated data, while the bias and RMSE helps to evaluate the level of discrepancy between simulations and observations. The impacts of LUCC on temperature in northeast

China were investigated by calculating the difference between the CTL and NE simulations.

3 Results

## 3.1 Analysis of the CTL simulations and their ensemble simulations

3.1.1 Mean temperature simulations during the 20-year period

The biases in the spatial pattern of annual mean temperature were calculated for every RCM and the two ensemble simulations (AEM and BMA) (Fig. 2). A cold bias was found in almost all of the grids in the WRF and RIEMS simulations, but in the RegCM3 simulations there were warm biases in the western parts of northeast China. The WRF simulations produced the highest biases, compared to the simulations of the other RCMs. The AEM ensemble simulations contained lower biases than single model simulations in most (over 80 %) grid cells. The BMA ensemble simulations produced lower biases than the AEM ones in 96 % of the grid cells. Not only did the BMA produce the lowest biases of all the simulations, but the bias was also lower than 2 °C in most grid cells (71 %). Thus, the BMA ensemble simulations produced the best results, out of the simulations tested, in northeast China (Fig. 2).

3.1.2 Performances of the RCMs and ensemble methods

The simulated temperature was significantly correlated with the observations in almost all of the grid cells within the study area for the three RCMs ($r > 0.421$, $n = 20$, $p < 0.05$; Fig. 3). The RegCM3 simulations obtained lower correlation coefficients in the central and northeastern parts of China compared to other regions, while the WRF model simulations had lower correlation coefficients in the northeastern and southeastern parts of China. The correlation coefficients between the RIEMS simulations and observation data were lower in the southern parts of China than in other parts.

The simulations of the three RCMs produced higher biases and RMSEs in the northern parts of China than in the southern parts, with RegCM3 producing lower biases and RMSEs than the other two RCMs. The higher biases of the RegCM3 simulations were found in parts of northeast China. The RIEMS simulations had higher biases in central parts than in other regions, while the WRF model produced higher biases and RMSEs in northeast China compared to other regions. Clearly, each RCM performed better in different regions.
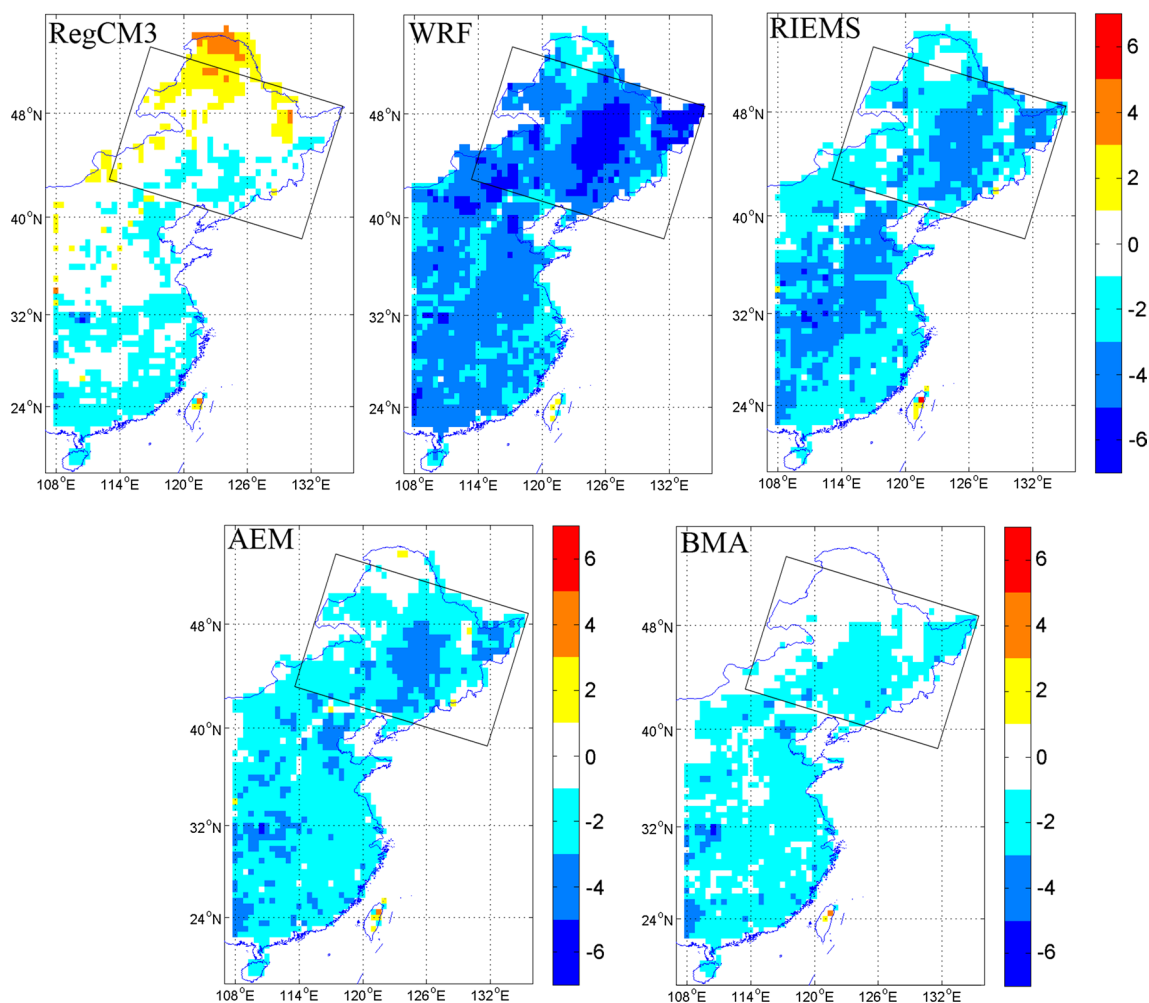
Fig. 2 Spatial patterns of the system biases of annual temperatures (°C; mean of 1981–2000)

The AEM and BMA ensemble simulations were both significantly correlated (*p* < 0.05) with observations in almost all of the grid cells, with correlation coefficients above 0.7 in most, and above 0.8 in more than half, of the cells (Fig. 3). In comparing the ensemble simulations' temperatures with those produced by the single-model simulations, the correlation coefficients were higher in most grid cells (>70 %) of the ensemble simulations. In particular, the correlation coefficients were improved in those grid cells where the single-model simulations had low correlation coefficients. Relatively low correlation coefficients were only found in parts of Shandong, Henan, and Heilongjiang provinces. The biases and RMSEs of the ensemble simulations' temperatures were lower than those of the single-model simulations; they were below 0.4 °C in the ensemble simulations. Moreover, the BMA simulations produced lower biases and RMSEs than the AEM simulations in over 55 % of the grid cells.

3.2 Effects of LUCC on the climate in northeast China, as simulated by the three RCMs and their ensemble simulations

3.2.1 Changes in annual mean temperature during the 20-year period

The LUCC in northeast China mainly comprised of an expansion of cropland and shrinkage of grassland and forest (Table 2). In the RegCM3 simulations, the annual temperature increased with a range of 0.05–0.15 °C, while the temperature decreased with a range of −0.1 to −0.4 °C in the WRF simulations (Fig. 4). However, the changes in the WRF simulated temperatures mainly occurred in the LUCC regions. In the RIEMS simulations, the temperature decreased in over 80 % of the grid cells and the range of variation in the RIEMS simulations was the largest of the three RCMs at between −0.5 and −1.5 °C. For the AEM
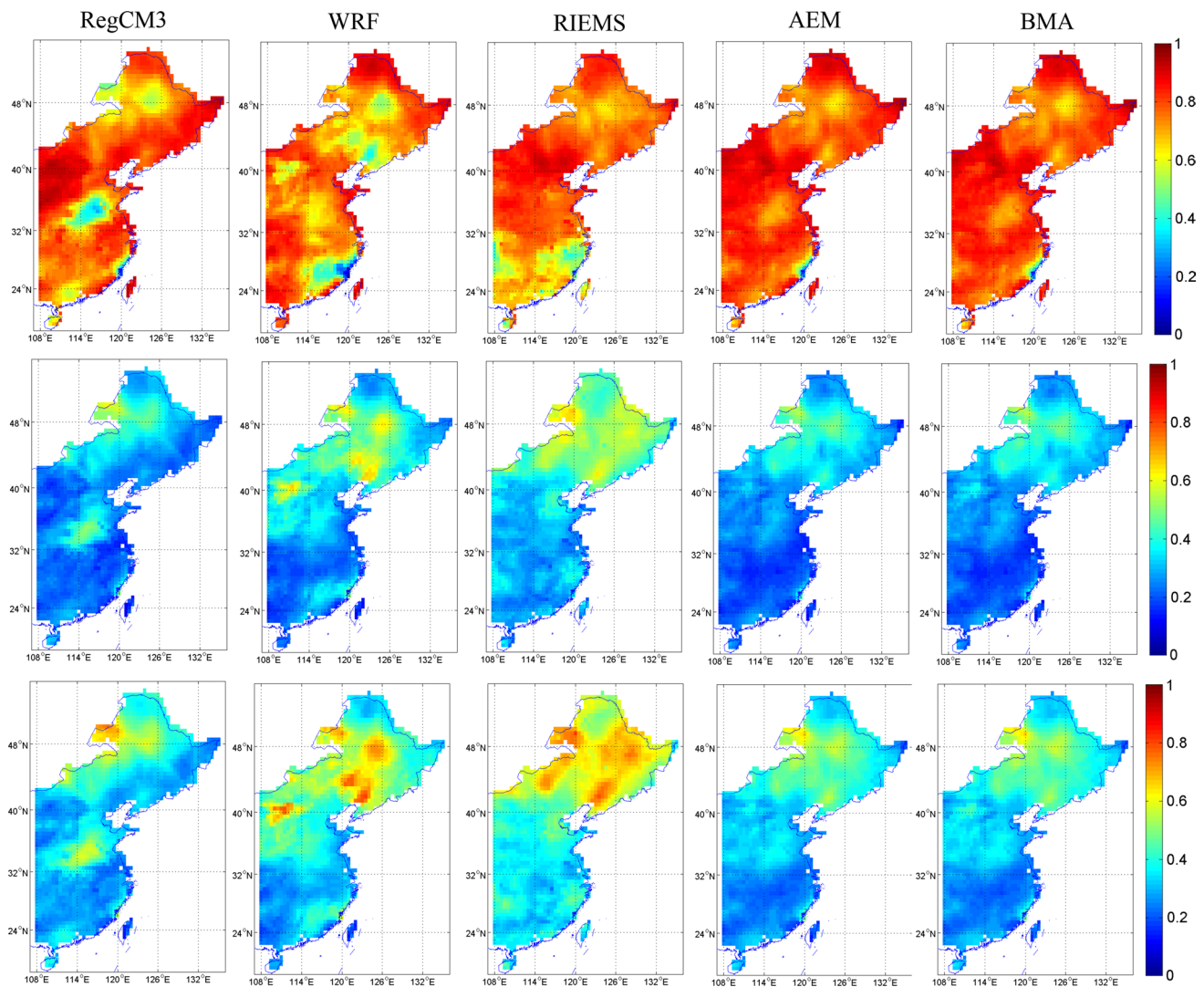
Fig. 3 Statistical results of the simulated annual temperature by the three RCMs (RegCM3, WRF and RIEMS) and their ensembles (AEM and BMA): correlation (*upper panels*); bias (*middle panels*, °C); and RMSE (*lower panels*)

Table 2 Changes in area of land use types during 1980–2000

| Land use type	Area of changed land use types (10^3 km^2)
Dryland cropland and pasture	56.7
Cropland/grassland mosaic	6.3
Cropland/woodland mosaic	23.4
Grassland	−12.6
Savanna	−22.5
Deciduous broadleaf forest	−7.2
Mixed forest	−34.2
Herbaceous wetland	−6.3
Barren or sparsely vegetated	−3.6

The negative numbers represent a reduction in area, while the positive numbers represent an increase in area

and BMA ensemble simulations, the temperature decreased by about 0.5 and 0.2 °C, respectively, in over 80 % of the grid cells.

3.2.2 The interannual variation of regional mean temperatures in the 20-year period

Over the 20-year period, the temperature decreased the most in the RIEMS simulations (−0.50 °C) compared to the other RCMs (Fig. 5). The WRF and RegCM3 simulated temperatures changed by between −0.05 and 0.1 °C over the 20-year study period. Although different trends were detected among each of the individual models, the ensemble AEM and BMA simulations showed that the regional mean temperature decreased over the past 20 years as a result of LUCC in northeast
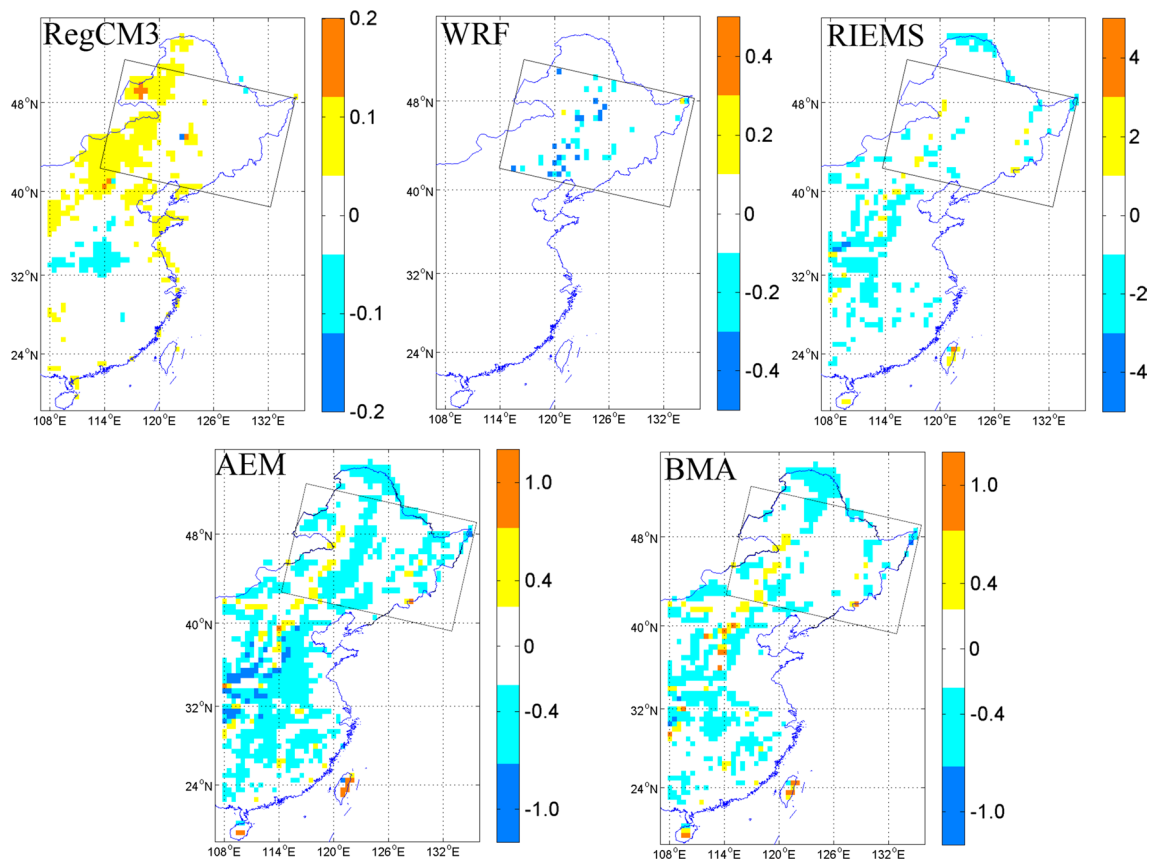
Fig. 4 Differences in annul mean temperature (°C) during the 20 years from 1981 to 2000 between the CTL and NE simulations

Fig. 5 Annual variation of regional mean temperature (°C) over the 20-year study period
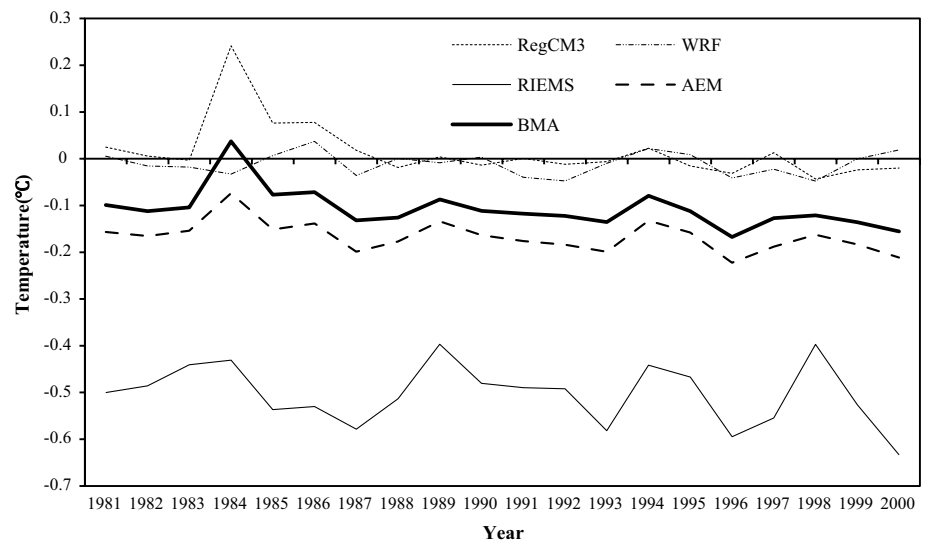
China. The AEM simulated temperature decreased more than the BMA temperature. Considering that the BMA ensemble CTL simulation produced the lowest biases of the CTL experiment simulations, the changes in the BMA simulated temperature were more similar to the observed changes in temperature. The changes in regional annual mean temperature of the BMA were around −0.11 °C.
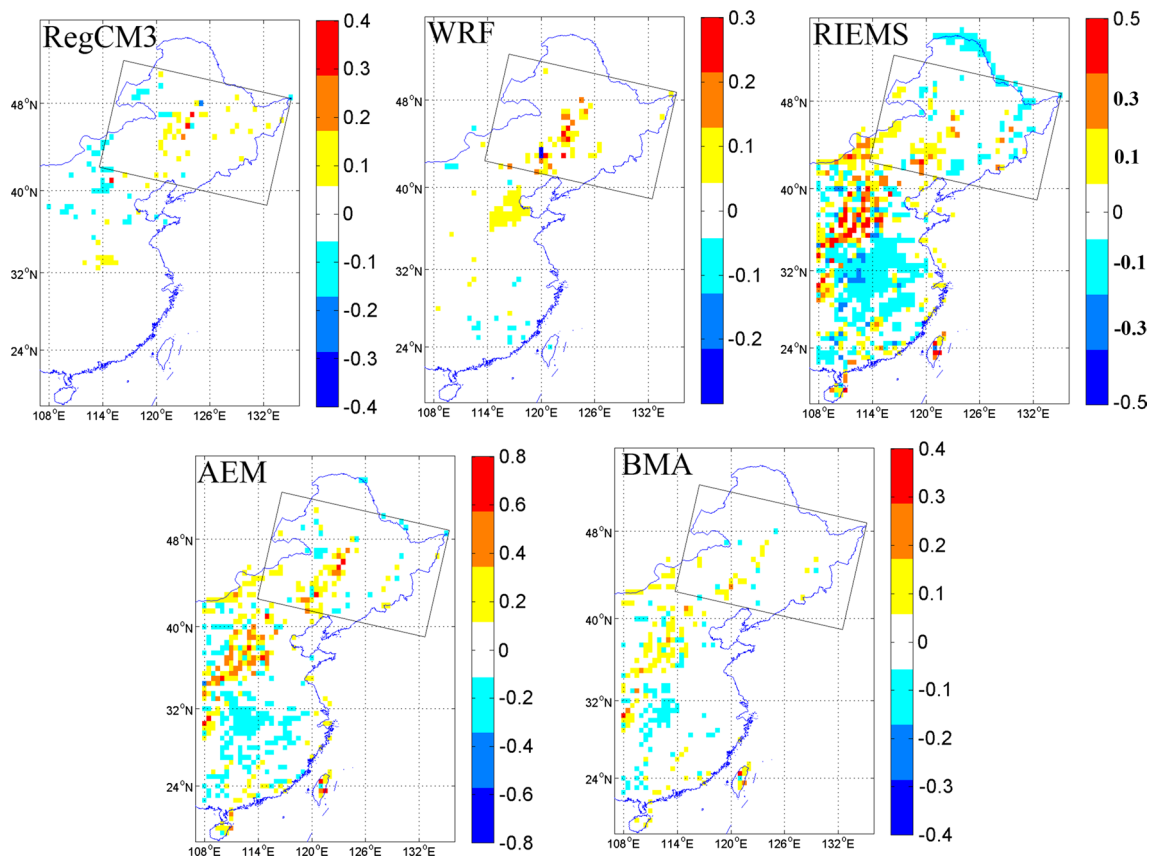
Fig. 6 The effects of LUCC on evapotranspiration (mm/day) as simulated by the three RCMs (RegCM3, WRF and RIEMS) and their ensemble simulations (AEM and BMA)

3.2.3 Changes in the surface energy budget during the 20-year period

An increase in evapotranspiration (ET) in northeast China was detected by the three RCMs. Evapotranspiration increased by around 0.1 mm/day in the RegCM3 and WRF simulations, while it increased by around 0.2 mm/day in the RIEMS simulations. The increase of ET in northeast China was also detected in the AEM and BMA simulations (Fig. 6); however, ET increased more in the AEM ensemble simulation than in the BMA one.

A decrease in net radiation NR as a result of LUCC was detected in northeast China by all three RCMs (Fig. 7); it decreased by around 3 W/m^2 in the RegCM3 and WRF simulations and 2 W/m^2 in the RIEMS simulation. There was an obvious decrease in NR in more regions of the RIEMS simulation than in the other two RCMs' simulations. The ensemble simulations of NR also showed that the NR decreased in response to LUCC in northeast China (Fig. 7); it decreased by 5 W/m^2 in the AEM simulations and 2 W/m^2 in the BMA simulations during the 20-year period.

4 Discussion and conclusion

In the present study, the effects of LUCC on climate were simulated by three RCMs (RegCM3, WRF and RIEMS) and the level of improvement attained by using ensemble methods was investigated. Two experiments (CTL and NE) were designed and run by the three models. The CTL experiment was used to compare the simulations of the different models and illustrated the improvements in results that were attained when using the ensemble methods. The NE experiment was designed to evaluate the effects of LUCC on the climate in northeast China, based on the three RCM simulations and their ensemble simulations.

The temperatures were simulated well by the three RCMs in the present study; however, their performances differed, depending on the specific region. For instance, RegCM3 performed better over southeast China, but worse over northeast China, in comparison to the simulations produced by RIEMS. Therefore, it is difficult to evaluate which model is the best at simulating the effects of LUCC on climate. This is in agreement with the results of many previous studies, in which it has been shown that the
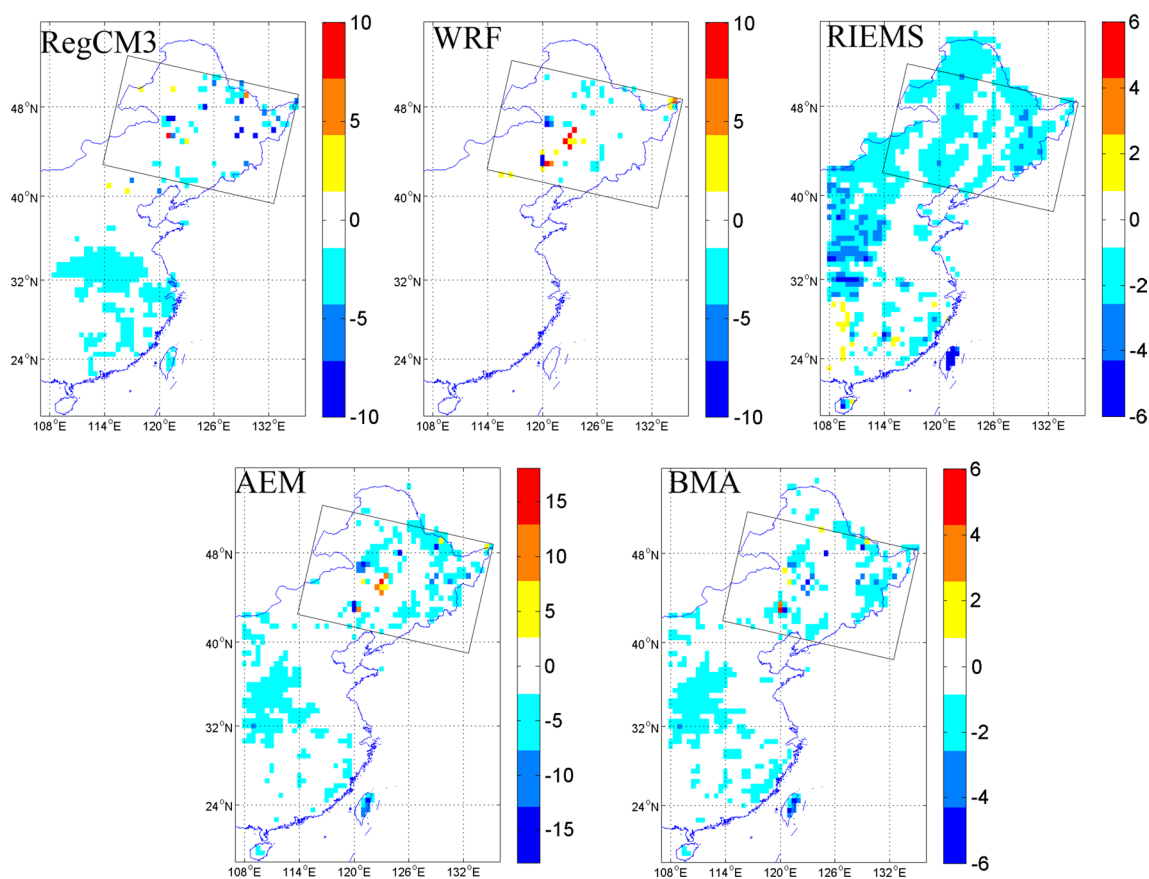
Fig. 7 The effects of LUCC on net radiation (W/m^2) as simulated by the three RCMs (RegCM3, WRF and RIEMS) and their ensemble simulations (AEM and BMA)

temperatures simulated by different RCMs produce different results (Déqué et al. 2012; Fu et al. 2005; Mearns et al. 2012). Therefore, large uncertainty exists in simulating the climate using any one RCM.

To circumvent this problem, ensemble methods were used to improve upon the simulations of each individual model. MME simulations have been proven to perform better than single models in many studies (e.g. Weisheimer et al. 2009; Annan and Hargreaves 2010). This is also evidenced by the results of the present study, in that the ensemble simulations had higher correlation coefficients and lower biases and RMSEs, when compared to observation data, than the single-model simulations. The improvement in the correlation coefficients was similar for the BMA and AEM simulations; however, the BMA simulations had lower biases and RMSEs than the AEM simulations. This suggests that the BMA simulation was more similar to the observation data, and therefore showed the best skill in simulating temperature.

The effects of LUCC on the climate in northeast China were investigated by comparing the CTL and NE simulations. An increase in the annual mean temperature was simulated by RegCM3 in the west of northeast China, while a decrease in annual mean temperature was produced in the RIEMS and WRF simulations. The opposing trend simulated by RegCM3, as compared to the other two RCMs, was probably caused by the high biases of RegCM3 in the west of northeast China. Therefore, in this region, the change in temperature may have been incorrectly simulated by RegCM3, which clearly demonstrates the problem of using any one RCM to simulate the effects of LUCC on climate.

The results of the CTL experiment showed that high biases existed in the individual model simulations, and the ensemble simulations had low biases, compared with the observations. The AEM method equally weighted the simulations of the three RCMs, while the BMA method gave higher weights to the RCM that performed better. In the NE experiment, the AEM simulation was dominated by the behavior of the RIEMS model. However, the BMA simulation integrated the simulations from the three models, so the changes in BMA simulated temperatures were more similar to the real temperature changes. This is in agreement with the results of the CTL experiment, which showed that the BMA simulation performed better than the AEM simulation.

The LUCC in northeast China during the 20-year study period mainly manifested in expanding cropland and shrinking grassland and forest areas. Pielke et al. (2007) showed that the effects of LUCC on climate varied with the changes in the conversion type, both spatially and temporally. Thus, it is difficult to explain the mechanisms when several different conversions between vegetation types occur (e.g., savanna to cropland, and mixed forest to cropland). However, quantitative results of LUCC were obtained by running the RCMs in the present study. Irrigation increased after land use changed from grassland and forest to cropland; as a result, more water was available, so the ET rates increased due to LUCC. This increase in ET brought heat from the surface to the upper atmosphere, leading to the decrease in temperature. In addition, NR decreases when forest is replaced by cropland, increasing the albedo (Betts 2000; Matthews et al. 2004; Jackson et al. 2008). Therefore, the temperature could also have decreased because of the decrease in NR. Thus, the LUCC in northeast China is likely to have indirectly caused the decrease in temperature observed. The effects of LUCC on climate in the NE experiment showed that the temperature decreased annually by about 0.11 °C in the BMA simulations. This is in agreement with other relevant studies on LUCC in China (Gao et al. 2007; Ge et al. 2014), and thus we can state that LUCC in northeast China has contributed to reducing the warming trend in eastern China.

In conclusion, the three different RCMs used in the present study simulated different effects of LUCC on the regional climate, even though the same LUCC was modeled. The ensemble of the RCM simulations produced better results than each RCM individually. Of the ensemble simulations, the BMA simulations performed better than the AEM simulations and provided the most similar results to the observations when simulating the effects of LUCC on climate. However, it is important to note the limitation that the effects of LUCC on climate were only simulated by three RCMs in this study; it took a large amount of time to run the three RCMs to simulate the effects of LUCC on climate over 20 years. Nevertheless, the ensemble results would have been more meaningful if more RCMs had been used. An extended study of this type should be carried out in future follow-up work.

References

Annan JD, Hargreaves JC (2010) Reliability of the CMIP3 ensemble. Geophys Res Lett 37:L02703. doi:10.1029/2009GL041994

Avissar R, Pielke RA (1989) A parameterization of heterogeneous land surfaces for atmospheric numerical models and its impact on regional meteorology. Mon Weather Rev 117:2113–2136

Bayes T (1763) An essay toward solving a problem in the doctrine of chances. Philos Trans R Soc 53:370–418

Betts RA (2000) Offset of the potential carbon sink from boreal forestation by decreases in surface albedo. Nature 408:187–190

Bounoua L, DeFries R, Collatz GJ, Sellers P, Khan H (2002) Effects of land cover conversion on surface climate. Clim Change 52:29–64

Cai M, Kalnay E (2004) Climate (communication arising): impact of land-use change on climate. Nature 427:214

Déqué M, Somot S, Sanchez-Gomez E, Goodess CM, Jacob D, Lenderink G, Christensen OB (2012) The spread amongst ENSEMBLES regional scenarios: regional climate models, driving general circulation models and interannual variability. Clim Dyn 38:951–964

Dickinson RE, Kennedy PJ, Henderson-Sellers A (1993) Biosphere-atmosphere transfer scheme (BATS) version 1e as coupled to the NCAR community climate model, vol. National Center for Atmospheric Research, Climate and Global Dynamics Division

Duan Q, Ajami NK, Gao X, Sorooshian S (2007) Multi-model ensemble hydrologic prediction using Bayesian model averaging. Adv Water Resour 30:1371–1386

Feng J, Wang Y, Ma Z, Liu Y (2013) Simulating the regional impacts of urbanization and anthropogenic heat release on climate across China. J Clim 25:7187–7203

Foley JA, DeFries R, Asner GP, Barford C, Bonan G, Carpenter SR, Chapin FS, Coe MT, Daily GC, Gibbs HK (2005) Global consequences of land use. Science 309:570–574

Fu C (2003) Potential impacts of human-induced land cover change on East Asia monsoon. Global Planet Change 37:219–229

Fu CB, Wei HL, Qian Y, Chen M (2000) Documentation on regional integrated environmental model system (RIEMS version 1). TEACOM science reports START Regional Committee for temperate East Asia, TSR.2000

Fu C, Wang S, Xiong Z, Gutowski WJ, Lee D, McGregor JL, Sato Y, Kato H, Kim J, Suh M (2005) Regional climate model intercomparison project for Asia. Bull Am Meteorol Soc 86:257–266

Gao X, Zhao Z, Filippo G (2002) Changes of extreme events in regional climate simulations over East Asia. Adv Atmos Sci 19:927–942

Gao X, Luo Y, Lin W, Zhao Z, Filippo G (2003) Simulation of effects of land use change on climate in China by a regional climate model. Adv Atmos Sci 20:583–592

Gao X, Zhang D, Chen Z, Pal JS, Giorgi F (2007) Land use effects on climate in China as simulated by a regional climate model. Sci China Earth Sci 50:620–628

Gates WL, Boyle JS, Covey C, Dease CG, Doutriaux CM, Drach RS, Fiorino M, Gleckler PJ, Hnilo JJ, Marlais SM (1999) An overview of the results of the Atmospheric Model Intercomparison Project (AMIP I). Bull Am Meteorol Soc 80:29–55

Ge Q, Zhang X, Zheng J (2014) Simulated effects of vegetation increase/decrease on temperature changes from 1982 to 2000 across the Eastern China. Int J Climatol 34:187–196

Giorgi F, Marinucci MR, Bates GT (1993a) Development of a second-generation regional climate model (RegCM2). Part I: boundary-layer and radiative transfer processes. Mon Weather Rev 121:2794–2813

Giorgi F, Marinucci MR, Bates GT, De Canio G (1993b) Development of a second-generation regional climate model (RegCM2). Part II: convective processes and assimilation of lateral boundary conditions. Mon Weather Rev 121:2814–2832

Giorgi F, Shields Brodeur C, Bates GT (1994) Regional climate change scenarios over the United States produced with a nested regional climate model. J Climate 7:375–399

Gutowski WJ Jr, Decker SG, Donavon RA, Pan Z, Arritt RW, Takle ES (2003) Temporal-Spatial Scales of Observed and Simulated Precipitation in Central US Climate. J Climate 16:3841–3847

Gutowski WJ Jr, Otieno FO, Arritt RW, Takle ES, Pan Z (2004) Diagnosis and attribution of a seasonal precipitation deficit in a US regional climate simulation. J Hydrometeoro l 5:230–242

Gutowski WJ, Arritt RW, Kawazoe S, Flory DM, Takle ES, Biner S, Caya D, Jones RG, Laprise R, Leung LR (2010) Regional extreme monthly precipitation simulated by NARCCAP RCMs. J Hydrometeorol 11:1373–1379

Hagedorn R, Doblas Reyes FJ, Palmer TN (2005) The rationale behind the success of multi-model ensembles in seasonal forecasting–I. Basic concept. Tellus A 57:219–233

Jackson RB, Randerson JT, Canadell JG, Anderson RG, Avissar R, Baldocchi DD, Bonan GB, Caldeira K, Diffenbaugh NS, Field CB (2008) Protecting climate with forests. Environ Res Lett 3:44006

Kalnay E, Cai M (2003) Impact of urbanization and land-use change on climate. Nature 423:528–531

Kiehl JT, Hack J, Bonan G, Boville B, Briegleb B, Williamson D, Rasch P (1996) Description of the NCAR community climate model (CCM3). In: NCAR Technical note NCAR/TN-420+ STR, 152 pp. Available from Publications Office of NCAR, PO Box 3000, Boulder, CO 80307

Kirtman BP, Min D (2009) Multimodel ensemble ENSO prediction with CCSM and CFS. Mon Weather Rev 137:2908–2930

Kirtman BP, Min D, Infanti JM, Kinter Iii JL, Paolino DA, Zhang Q, van den Dool H, Saha S, Mendez MP, Becker E (2013) The North American Multi-Model Ensemble (NMME): phase-1 seasonal to interannual prediction, phase-2 toward developing intraseasonal prediction. Bull Am Meteorol Soc 95:585–601

Liu J, Liu M, Deng X, Zhuang D, Zhang Z, Luo Di (2002) The land use and land cover change database and its relative studies in China. J Geogr Sci 12:275–282

Liu J, Liu M, Zhuang D, Zhang Z, Deng X (2003) Study on spatial pattern of land-use change in China during 1995–2000. Sci China Earth Sci 46:373–384

Liu J, Liu M, Tian H, Zhuang D, Zhang Z, Zhang W, Tang X, Deng X (2005) Spatial and temporal patterns of China's cropland during 1990–2000: an analysis based on Landsat TM data. Remote Sens Environ 98:442–456

Matthews HD, Weaver AJ, Meissner KJ, Gillett NP, Eby M (2004) Natural and anthropogenic climate change: incorporating historical land cover change, vegetation dynamics and the global carbon cycle. Clim Dyn 22:461–479

McGuffie K, Henderson-Sellers A, Zhang H, Durbidge TB, Pitman AJ (1995) Global climate sensitivity to tropical deforestation. Global Planet Change 10:97–128

Mearns LO, Arritt R, Biner S, Bukovsky MS, McGinnis S, Sain S, Caya D, Correia J Jr, Flory D, Gutowsky W (2012) The north American regional climate change assessment program. Bull Am Meteorol Soc 93:1337–1362

Nobre CA, Sellers PJ, Shukla J (1991) Amazonian deforestation and regional climate change. J Climate 4:957–988

Pal JS, Giorgi F, Bi X, Elguindi N, Solmon F, Rauscher SA, Gao X, Francisco R, Zakey A, Winter J (2007) Regional climate modeling for the developing world: the ICTP RegCM3 and RegCNET. Bull Am Meteorol Soc 88:1395–1409

Pielke RA (2005) Land use and climate change. Science 310:1625–1626

Pielke RA, Marland G, Betts RA, Chase TN, Eastman JL, Niles JO, Running SW (2002) The influence of land-use change and landscape dynamics on the climate system: relevance to climate-change policy beyond the radiative effect of greenhouse gases. Philos Trans R Soc A 360:1705–1719

Pielke RA, Adegoke J, Beltran Przekurat A, Hiemstra CA, Lin J, Nair US, Niyogi D, Nobis TE (2007) An overview of regional land-use and land-cover impacts on rainfall. Tellus B 59:587–601

Raftery AE, Gneiting T, Balabdaoui F, Polakowski M (2005) Using Bayesian model averaging to calibrate forecast ensembles. Mon Weather Rev 133:1155–1174

Reifen C, Toumi R (2009) Climate projections: Past performance no guarantee of future skill? Geophys Res Lett 36:L13704. doi:10.1029/2009GL038082

Shi W, Wang H (2003) The regional climate effects of replacing farmland and re-greening the desertification lands with forest or grass in west China. Adv Atmos Sci 20:45–54

Sloughter JM, Raftery AE, Gneiting T, Fraley C (2007) Probabilistic quantitative precipitation forecasting using Bayesian model averaging. Mon Weather Rev 135:3209–3220

Suh MS, Lee DK (2004) Impacts of land use/cover changes on surface climate over east Asia for extreme climate cases using RegCM2. J Geo Res 109

Tian H, Melillo JM, Kicklighter DW, Pan S, Liu J, McGuire AD, Moore B III (2003) Regional carbon dynamics in monsoon Asia and its implications for the global carbon cycle. Global Planet Change 37:201–217

Tian H, Lu C, Chen G, Xu X, Liu M, Ren W, Tao B, Sun G, Pan S, Liu J (2011) Climate and land use controls over terrestrial water use efficiency in monsoon Asia. Ecohydrology 4:322–340

Trenberth KE (2004) Climatology (communication arising): rural land-use change and climate. Nature 427:213

Wang Y, Sen OL, Wang B (2003) A highly resolved regional climate model (IPRC-RegCM) and its simulation of the 1998 severe precipitation event over China. Part I: model description and verification of simulation. J Climate 16:1721–1738

Wang H, Shi W, Chen X (2006) The statistical significance test of regional climate change caused by land use and land cover variation in West China. Adv Atmos Sci 23:355–364

Wang S, Fu C, Wei H, Qian Y, Xiong Z, Feng J, Zhao D, Dan L, Han Z, Su B (2013) Regional integrated environmental modeling system: development and application. Clim Change. doi:10.1007/s10584-013-0973-3

Wang Y, Feng J, Gao H (2014) Numerical simulation of the impact of land cover change on regional climate in China. Theor Appl Climatol 115:141–152

Weisheimer A, Doblas Reyes FJ, Palmer TN, Alessandri A, Arribas A, Déqué M, Keenlyside N, MacVean M, Navarra A, Rogel P (2009) ENSEMBLES: a new multi-model ensemble for seasonal-to-annual predictions—Skill and progress beyond DEMETER in forecasting tropical Pacific SSTs. Geophys Res Lett 36:L21711

Xiong Z, Fu C, Zhang Q (2006) On the ability of the regional climate model RIEMS to simulate the present climate over Asia. Adv Atmos Sci 23:784–791

Xue Y (1996) The impact of desertification in the Mongolian and the Inner Mongolian grassland on the regional climate. J Climate 9:2173–2189

Xue Y, Shukla J (1993) The influence of land surface properties on Sahel climate. Part 1: desertification. J Climate 6:2232–2245

Zhang H, Gao X (2009) On the atmospheric dynamical responses to land-use change in East Asian monsoon region. Clim Dyn 33:409–426

Zhang X, Yan X (2014) A novel method to improve temperature simulations of general circulation models based on ensemble empirical mode decomposition and its application to multi-model ensembles. Tellus A 66:24846

Zhang X, Yan X (2015) A new statistical precipitation downscaling method with Bayesian model averaging: a case study in China. Clim Dyn. doi:10.1007/s00382-015-2491-7

Zhang H, Henderson-Sellers A, McGuffie K (1996) Impacts of tropical deforestation. Part I: process analysis of local climatic change. J Clim 9:1497–1517

Zhang H, Henderson-Sellers A, McGuffie K (2001) The compounding effects of tropical deforestation and greenhouse warming on climate. Clim Change 49:309–338

Zhang J, Dong W, Wu L, Wei J, Chen P, Lee D (2005) Impact of land use changes on surface warming in China. Adv Atmos Sci 22:343–348

Zhang J, Wu L, Dong W (2011) Land–atmosphere coupling and summer climate variability over East Asia. J Geophys Res 116:D05117. doi:10.1029/2010JD014714

Zhao D (2013) Performance of regional integrated environment modeling system (RIEMS) in precipitation simulations over east Asia. Clim Dyn 40:1767–1787